Engineering Structures 293 (2023) 116654

Contents lists available at ScienceDirect

Engineering Structures

journal homepage: www.elsevier.com/locate/engstruct

A member redundancy index based on distributed static indeterminacy for optimum material distribution for structures with axially loaded members

Nader M. Okasha [a,*], Mohamed Soliman [b], Sunyong Kim [c], Dan M. Frangopol [d], Abdel Kareem Alzo'ubi [a]

[a] Department of Civil Engineering, College of Engineering, Abu Dhabi University, P.O. Box:1790, Al Ain, United Arab Emirates
[b] School of Civil and Environmental Engineering, Oklahoma State University, Stillwater, OK 74078, USA
[c] Department of Civil and Environmental Engineering, Wonkwang University, 460 Iksandae-ro, Iksan, Jeonbuk 54538, Republic of Korea
[d] Fazlur R. Khan Endowed Chair of Structural Engineering and Architecture, Department of Civil and Environmental Engineering, ATLSS Engineering Research Center, Lehigh University, 117 ATLSS Dr., Bethlehem, PA 18015-4729, USA

ARTICLE INFO

Keywords:
Material distribution
Redundancy matrix
Member redundancy index
Static indeterminacy distribution
Structural systems
Structural redundancy
Indeterminacy

ABSTRACT

Redundancy analysis in structural systems has been typically approached under particular loading conditions. Structural systems that are found to provide adequate levels of redundancy in light of such an approach may face serious threats resulting from accidental loads. Additionally, determining the degree of redundancy of a system as one unique global information ignores the spatial distribution of the redundancy in that system. Improper distribution of redundancy in the system may lead to the presence of superfluous material in parts of the system. One system measure that has been widely used to gage the level of redundancy in structures is the static indeterminacy. Hence, the redundancy matrix is an excellent tool that provides valuable insight into the distribution of the static indeterminacy among the structural members in the system; independently from any loads applied to the system. One of the essential components in the redundancy matrix is the distributed static indeterminacy. While providing satisfactory levels of redundancy in a system is encouraged, it is also necessary to optimize the material distribution in the system. Having members in the system that are highly, or even completely, redundant indicates an inefficient distribution of material and should be avoided. In this paper, a member redundancy index based on the distributed static indeterminacy is derived. This index can be used to efficiently distribute the material in the system in order to optimize its redundancy distribution.

1. Introduction

Ensuring a satisfactory degree of redundancy in structural systems is evidently important; in order to provide adequate levels of assurance against the collapse of the system in the event of losing one or more of its members, partially or completely [1-3]. Integrating the concepts of redundancy in design and maintenance is regarded as an effective way of optimizing structures, since it reflects the geometric and topological configuration of structures [4]. As a result, savings in material by its proper distribution in the system can be achieved [5].

A commonly used conventional definition of redundancy is the degree of static indeterminacy of the structural system [6]. However, Frangopol and Curley [7] demonstrated how the degree of static indeterminacy by itself does not constitute an adequate measure of the overall system behavior as it overlooks the member contributions to the system behavior. All the well-established methods of determining the degree of static indeterminacy dating back to Maxwell [8], and more recently in Pellegrino and Calladine [9], unfortunately, provide little to no information about the spatial distribution of static indeterminacy [10].

Even though a system should possess a high degree of redundancy, it is not desirable to have members that are highly redundant because that indicates the presence of material that is inefficiently, or even unnecessarily, allocated in the system. It is therefore necessary to establish indicators that efficiently measure the importance and contribution of each member to the overall system redundancy, the sensitivity of the system to the material distribution in the system, and the optimum amount of material that should be allocated to each member. Such information can be effectively utilized in the design of new structures, and in the repair, maintenance, and replacement of members of existing ones.

* Corresponding author.
E-mail address: nader.okasha@adu.ac.ae (N.M. Okasha).

https://doi.org/10.1016/j.engstruct.2023.116654
Received 5 March 2023; Received in revised form 4 July 2023; Accepted 22 July 2023
Available online 28 July 2023
0141-0296/© 2023 Elsevier Ltd. All rights reserved.

Nomenclature

γ_i	Diagonal entry of the redundancy matrix, $R_{i,i}$
$\gamma_i^i(a)$	Distributed static indeterminacy (DSI) for member i when its cross-sectional area is set to $A_i = a$
$\gamma_j^i(a)$	DSI for members $j \neq i$ when the cross-sectional area, A_i, of member i is set to an arbitrary value, a, which is the j^{th} element in the diagonal of the redundancy matrix, **R**, when the i^{th} member has an area of a.
$\delta_j^i(a)$	Change in the DSI for member j when A_i changes from zero to a
θ_i^j	Constant that relates the change in the DSI for member i to that of member j as A_i varies
$\rho_i(A_i)$	Member redundancy index (MRI) for all members of the system w.r.t. to introducing member i in the system
$\rho_j^i(A_i)$	MRI for member j w.r.t. to introducing member i in the system
τ_{50}^i	Target area A_i for member i that causes $\rho_i(A_i)$ to be 50 %.
$\mathbf{A}$	Equilibrium matrix
A_i	Cross-sectional area of member i
$\mathbf{B}$	Compatibility matrix
$\mathbf{d}$	Joint displacement vector
$\mathbf{e}_0$	Initial member elongation vector
$\mathbf{e}_{elastic}$	Elastic member elongation vector
E_i	Modulus of elasticity of member i
$\mathbf{e}_{total}$	Total member elongation vector
F	An external force applied to a structure (Fig. 1).
$\mathbf{F}$	External force vector
$\mathbf{f}$	Internal force vector
$f_{1,j}$	Internal force in the member connected between nodes 1 and j
$F_{x,1}$	Components of force F applied to Node 1 in the x direction
$F_{y,1}$	Components of force F applied to Node 1 in the y direction
$F_{z,1}$	Components of force F applied to Node 1 in the z direction
$\mathbf{G}$	Diagonal matrix of axial stiffness, in which $G_{ii} = A_iE_i/L_i$
$l_{1,j}$	Length of the member connected between nodes 1 and j
L_i	Length of member i.
$\mathbf{R}$	Redundancy matrix
x_i	x coordinate of node i
y_i	y coordinate of node i
z_i	z coordinate of node i

Little in the literature has focused on theoretical studies regarding distributed indeterminacy [11]. The concept of the redundancy matrix was presented in several studies as a basis for offering additional insight into system properties and distributed indeterminacy [10]. The redundancy matrix describes the system behavior with no regard to the loading conditions and is purely based on the inherent performance of the structure, including its geometric configuration, material properties, and member stiffnesses [12,13]. The unpredictability of accidental loads makes it necessary to quantify the redundancy as such [14]. The first version of the redundancy matrix appeared in Linkwitz [15], where it was recognized as an idempotent matrix. Ströbel and Singer [16] proposed the concepts of elastic redundancy and geometric redundancy in an attempt to study distributed indeterminacy. Wagner [17] conducted a redundancy analysis on cable structures and truss structures using similar concepts. Tibert [18,19], Eriksson and Tibert [20] and Zhou *et al.* [11] presented analytical methods to determine the distributed static indeterminacy (DSI). The redundancy matrix was also used to evaluate structural sensitivity and robustness [11,14,16,18–26].

Interactive designs require multiple calculations of the redundancy matrix, which can be computationally expensive. In order to replace the recalculation of the redundancy matrix by a simpler updating procedure that enables faster optimization loops, Krake *et al.* [27] proposed generic algebraic formulations for efficiently updating the redundancy matrix. Gade *et al.* [28] extended the concept of discrete redundancy matrices to redundancy operators in continuous representations of structures.

Although the redundancy matrix and the DSI can provide relative measures of the redundancy of members in a structural system, the values they offer provide little information regarding the material distribution in the system. In order to use these concepts in design optimization, maintenance, repair, or replacement during the life-cycle of a structure, it is important to have an indicator that measures the system redundancy caused by a given material distribution versus the loss of one of the members. In this paper, the mathematical derivation for such an indicator, namely the Member Redundancy Index (MRI) will be proposed. It will also be shown how this index can be used to establish target material distributions that satisfy desired levels of system redundancy with efficient material distribution.

2. Redundancy matrix

The derivation of the equation for the redundancy matrix can be illustrated in the example of the 3D system shown in Fig. 1. Node 1 is connected to four neighboring nodes (2, 3, 4, 5) by four axial members and an external force F is applied to the system at Node 1. The equilibrium equations that relate the internal forces in the members to the cartesian components of the external force F can be written in matrix form as follows [29].

$$\begin{bmatrix} \frac{(x_1-x_2)}{l_{1,2}} & \frac{(x_1-x_3)}{l_{1,3}} & \frac{(x_1-x_4)}{l_{1,4}} & \frac{(x_1-x_5)}{l_{1,5}} \\ \frac{(y_1-y_2)}{l_{1,2}} & \frac{(y_1-y_3)}{l_{1,3}} & \frac{(y_1-y_4)}{l_{1,4}} & \frac{(y_1-y_5)}{l_{1,5}} \\ \frac{(z_1-z_2)}{l_{1,2}} & \frac{(z_1-z_3)}{l_{1,3}} & \frac{(z_1-z_4)}{l_{1,4}} & \frac{(z_1-z_5)}{l_{1,5}} \end{bmatrix} \begin{bmatrix} f_{1,2} \\ f_{1,3} \\ f_{1,4} \\ f_{1,5} \end{bmatrix} = \begin{bmatrix} F_{x,1} \\ F_{y,1} \\ F_{z,1} \end{bmatrix} \quad (1)$$

where x_i, y_i, and z_i are the 3D coordinates of node $i = 1, 2, \ldots 5$, $f_{1,j}$ is the internal force in the member connected between nodes 1 and j, $l_{1,j}$ is the length of the member connected between nodes 1 and j, such that $j = 2, 3, 4, 5$, and $F_{x,1}$, $F_{y,1}$, and $F_{z,1}$ are the components of the force F applied to Node 1 in the x,y, and y directions, respectively.

By applying the concepts in Equation (1) to all the joints and bars comprising a system, the equilibrium equation is written as follows.

$$\mathbf{Af} = \mathbf{F} \quad (2)$$

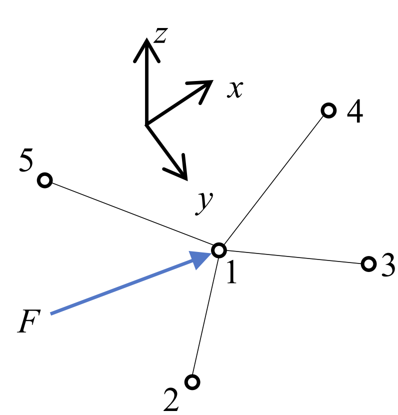

Fig. 1. An illustrative example of a structure with four members connected at a Node.

where $\mathbf{A}$ is the equilibrium matrix, $\mathbf{f}$, and $\mathbf{F}$ are the internal and external force vectors, respectively.

By minimizing the total complete system potential energy function with respect to different variables produces the compatibility, and constitutive equations shown in Equations (3) and (4), respectively [14].

$$\mathbf{Bd} = \mathbf{e}_{total} \tag{3}$$

$$\mathbf{Ge}_{elastic} = \mathbf{f} \tag{4}$$

where $\mathbf{B}$ is the compatibility matrix, $\mathbf{d}$ is the (infinitesimal) joint displacement vector, $\mathbf{e}_{total}$ and $\mathbf{e}_{elastic}$ are the total and elastic member elongation vectors, respectively, and $\mathbf{G}$ is a diagonal matrix of axial stiffness, in which $G_{ii} = A_iE_i/L_i$, such that A_i, E_i, and L_i are the cross-sectional area, modulus of elasticity, and length of member i, respectively. The compatibility matrix, $\mathbf{B}$, is related to the equilibrium matrix, $\mathbf{A}$, as follows [30].

$$\mathbf{B} = \mathbf{A}^T \tag{5}$$

The total elongation $\mathbf{e}_{total}$ can be decomposed into the elastic part $\mathbf{e}_{elastic}$, which is caused by the force $\mathbf{F}$, and an initial part $\mathbf{e}_0$, which is usually caused by fabrication error or thermal strains [31].

$$\mathbf{e}_{total} = \mathbf{e}_{elastic} + \mathbf{e}_0 \tag{6}$$

Substituting Equation (3) in Equation (6) and then in Equation (4) to provide.

$$\mathbf{G}(\mathbf{Bd} - \mathbf{e}_0) = \mathbf{f} \tag{7}$$

Substituting Equations (5) and (7) in Equation (2) to obtain.

$$(\mathbf{AGA}^T)\mathbf{d} - \mathbf{AGe}_0 = \mathbf{F} \tag{8}$$

which can be solved for the unknown displacements, $\mathbf{d}$ as follows.

$$\mathbf{d} = \left(\mathbf{AGA}^T\right)^{-1}[\mathbf{F} + \mathbf{AGe}_0] \tag{9}$$

Since the redundancy distribution is a structural property that is independent of the external loads, only the part that is independent of $\mathbf{F}$ is considered [10]. Now, by substituting Equations (5) and (9) in Equation (3) then substituting the result in Equation (6) gives.

$$\mathbf{e}_{elastic} = \left[\mathbf{A}^T\left(\mathbf{AGA}^T\right)^{-1}\mathbf{AG} - \mathbf{I}\right]\mathbf{e}_0 = -\mathbf{Re}_0 \tag{10}$$

where $\mathbf{R}$ is known in the literature as the redundancy matrix [10,11,14,20] because it maps the initial elongations, $\mathbf{e}_0$, to the negative elastic elongations, $\mathbf{e}_{elastic}$, and is determined as.

$$\mathbf{R} = \mathbf{I} - \mathbf{A}^T\left(\mathbf{AGA}^T\right)^{-1}\mathbf{AG} \tag{11}$$

The redundancy matrix, $\mathbf{R}$, in Equation (10) can be interpreted as the response of a member due to an initial 'unit' elongation. In Equation (10), $\mathbf{e}_0$ can be viewed as the prescribed initial elongation of the unconstrained member before assembly, and $\mathbf{e}_{elastic}$ is the elastic part of the resulting elongation. In this manner, the redundancy matrix, $\mathbf{R}$, in Equation (10) describes the constraint of the surrounding structure on the members of the system. Furthermore, the trace of the redundancy matrix, $\mathbf{R}$, is equal to the degree of static indeterminacy [20].

3. Distributed static indeterminacy

The diagonal entry of the redundancy matrix, $\gamma_i = R_{i,i}$, demonstrates the contribution of member i to the degree of static indeterminacy and is called the Distributed Static Indeterminacy (DSI) of member i [11,14,20]. The range of each DSI is between zero and one [11]. A value of $\gamma_i = 1.0$ indicates that element i is restrained from elongation because it is either fixed between two rigid supports, or surrounded by infinitely stiffer members in the system. Thus, an element i with $\gamma_i = 1.0$ is said to have a high degree of redundancy, i.e. its removal from the system will cause no effects on its load-bearing behavior. On the contrary, when $\gamma_i =$ 0.0, element i is free to elongate. The low redundancy for this element highlights its importance to the structure, which will (partially) fail if this element is removed. Smaller values for γ_i indicate that a fabrication error in member i will lead only to small forces in the structure. On the other hand, higher values for γ_i indicate that elongations in member i will cause larger forces [10].

4. Effect of material distribution on DSI

In order to study the effect of material distribution in a structure on the DSI of its members, the cross-sectional area of one member can be varied while the remaining members have their cross-sectional areas unchanged. Accordingly, the MRI is formulated with respect to the member having its cross-sectional area varied.

When the cross-sectional area, A_i, of member i is set to an arbitrary value a, the DSI for members $j \neq i$ in the system will be denoted as $\gamma_j^i(a)$, which is the j^{th} element in the diagonal of the redundancy matrix, $\mathbf{R}$, when the i^{th} member has an area of a. Also, the DSI for member i itself when its cross-sectional area is set to $A_i = a$ will be denoted as $\gamma_i^i(a)$.

As the value of A_i varies between zero and infinity, some observations regarding the DSI values can be intuitively expected. As A_i is reduced, the stiffness of member i is decreased relative to the remaining members in the system. When A_i approaches zero, the stiffness of the surrounding members becomes infinitely larger than that of member i. Therefore, elongation of member i is restricted and its DSI when $A_i =$ 0 should be $\gamma_i^i(0) = 1.0$. This indicates that member i is redundant to the system if its cross-sectional area is zero and can be removed or ignored since it does not contribute to the static indeterminacy of the system. On the other hand, when A_i is increased and approaches infinity, the stiffness of member i becomes infinitely larger than the surrounding members. Accordingly, these surrounding members can no longer restrain the elongations that may develop in member i. In such case, one can expect that $\gamma_i^i(\infty) = 0.0$. This value indicates that member i is not redundant and its removal from the system can be detrimental to the system. Hence as A_i is increased from 0 to ∞, the value of $\gamma_i^i(A_i)$ decreases from 1.0 to 0 as depicted in the sketch shown in Fig. 2(a). Clearly, despite the rational basis for the preceding observation, achieving maximum levels of member redundancy by providing an infinitely large cross-section to a member is feasibly unacceptable. Accordingly, the DSI cannot be used in such form in material distribution optimization.

The intuitive prediction of the values of the remaining members in the system is not as simple. However, each of the remaining members in the system $j \neq i$ will have a value $\gamma_j^i(0)$ that corresponds to its DSI if member i did not exist in the system, i.e., $A_i = 0$. On the other hand, each of the remaining members $j \neq i$ will have a value $\gamma_j^i(\infty)$ that corresponds to its DSI if member i has infinite cross-sections, i.e., $A_i = \infty$. As will be explained next, the values $\gamma_j^i(0)$ and $\gamma_j^i(\infty)$ are the two minimum and maximum extremes for $\gamma_j^i(A_i)$, respectively, for member j as A_i varies. The variation in $\gamma_j^i(A_i)$ from $\gamma_j^i(0)$ to $\gamma_j^i(\infty)$ is depicted in Fig. 2(b).

Fig. 2(a) and (b) showed a difference in the redundancy of the members when the cross-sectional area of one of the members, i, becomes infinitely large, $A_i = \infty$. First, the same member i becomes too strong to be restrained by the remaining members in the system. Accordingly, member i cannot be removed from the system and thus its redundancy is $\gamma_i^i(\infty) = 0$. Second, the redundancy of a different member j in such a case cannot be predicted as easily. This is because the sum of the redundancy of the remaining members in the system, $j \neq i$, is equal to the degree of static indeterminacy of the system. For any member, $j \neq i$, the redundancy in such a case is then equal to the DSI of that member when $A_i = \infty$, which can be any value between 0.0 and 1.0.

The change in the DSI denoted here as $\delta_j^i(a)$, for member j when A_i changes from zero to a can be calculated as.

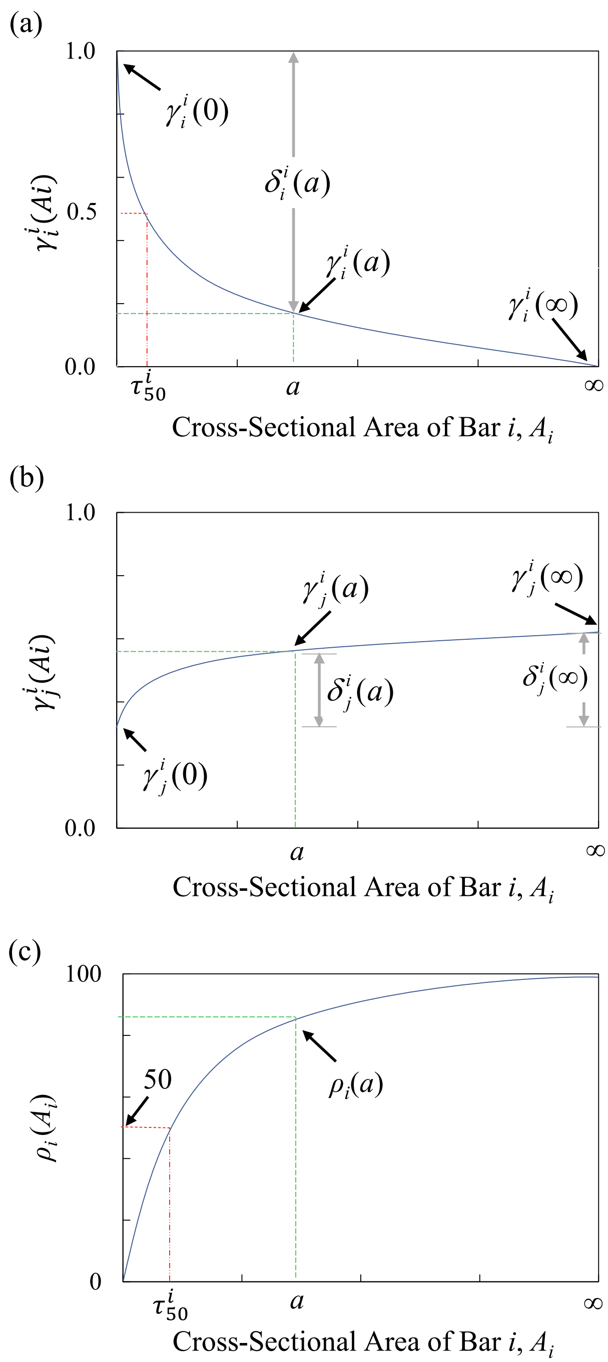

Fig. 2. A graphical depiction of the variation in DSI w.r.t the change in cross-section of member i, A_i for: (a) Member i, $\gamma_i^i(A_i)$, (b) Member $j \neq i$, $\gamma_j^i(A_i)$, and (c) variation of the MRI w.r.t. A_i.

$$\delta_j^i(a) = \gamma_j^i(a) - \gamma_j^i(0) \tag{12}$$

The change in DSI for member i, $\delta_i^i(a)$ can be calculated in a similar manner. Accordingly, the maximum change in the DSI, $\delta_j^i(\infty)$, for member j when A_i changes from zero to ∞ can be calculated as.

$$\delta_j^i(\infty) = \gamma_j^i(\infty) - \gamma_j^i(0) \tag{13}$$

The magnitude of $\delta_j^i(\infty)$ can be interpreted as the maximum gain in redundancy for member j if member i is introduced to the system. The changes in DSI, $\delta_i^i(A_i)$ and $\delta_j^i(A_i)$, with changing A_i are illustrated in Fig. 2 (a) and (b), respectively.

If a system of n members is indeterminate to the first degree in the presence of member i, then it should be expected that $\gamma_j^i(0) = 0$, because the system without member i is statically determinate and $\sum_{j\neq i}^{n}\gamma_j^i(0) =$ the degree of static indeterminacy of the system without member i, which is equal to 0 in this case, and $\gamma_j^i(0)$ cannot be negative for any $j \neq i$. However, if the system is indeterminate to a degree of two or more, the value of $\gamma_j^i(0)$ can be any value between 0.0 and 1.0. In addition, since $\sum_j^n \gamma_j^i(A_i) =$ the degree of static indeterminacy of the system, which is constant regardless of the material distribution in the system, the reduction in $\gamma_i^i(A_i)$, i.e $\delta_i^i(A_i)$, will be distributed to the remaining members and thus $\delta_j^i(A_i)$ and therefore $\gamma_j^i(A_i)$ will increase. Accordingly, the following equation must be valid.

$$\left|\delta_i^i(A_i)\right| = \sum_{j\neq i}^{n} \delta_j^i(A_i) \tag{14}$$

In other words, the DSI of each member j receives a fraction of the DSI lost by member i. Therefore, as the importance of member i increases by increasing its A_i, the importance of the remaining members $j \neq i$ decreases in the system relatively. The absolute value on the left side of Equation (14) is used since the magnitude of the change $\delta_i^i(A_i)$ is what is relevant (note that $\delta_i^i(A_i)$ is always negative while $\delta_j^i(A_i)$ is always positive). In some cases, as will be shown in the following examples, $\gamma_j^i(A_i)$ may remain constant, i.e., $\delta_j^i(A_i) = 0$, for some members as A_i increases. This occurs when member i has no bearing on the restraint of member j.

Since the values of $\gamma_j^i(A_i)$ and $\gamma_i^i(A_i)$ result from solutions of the same linear system where only one parameter is varied, namely the cross-sectional area of member i, and given the constraint in Equation (14), it can be concluded that $\delta_j^i(A_i)$ is proportional to $\delta_i^i(A_i)$ and the following equation is valid.

$$\delta_j^i(A_i) = \theta_j^i \delta_i^i(A_i) \tag{15}$$

where θ_j^i is a constant that relates the change in the DSI for member i to that of member j as A_i varies. Similarly, the DSI's of any two members j and k are also proportional and related as follows.

$$\delta_j^i(A_i) = \theta_j^k \delta_k^i(A_i) \tag{16}$$

where θ_j^k is a constant that relates the change in the DSI for member k to that of member j as A_i varies.

As was previously explained, a member i with $A_i = 0$ can be deemed to be redundant in a system and its DSI is at the maximum value of 1.0. However, member i having $A_i = a$ can be viewed to have lost an amount in its DSI from its maximum value of 1.0, which is equivalent to $\delta_i^i(a) = \gamma_i^i(a) - \gamma_i^i(0) = \gamma_i^i(a) - 1.0$, as shown in Fig. 2(a). To maintain the same degree of static indeterminacy, this $\delta_i^i(a)$ loss must be distributed to the remaining members. Accordingly, the presence of member i having $A_i = a$ in the system will cause a member j to gain an amount to its DSI equivalent to $\delta_j^i(a) = \gamma_j^i(a) - \gamma_j^i(0)$, as shown in Fig. 2(b). The magnitude of $\delta_j^i(a)$ is the difference in the DSI of member j between having member i with $A_i = a$ in the system and not having member i in the system. At this stage, it is apparent that introducing a new member into a system or increasing the cross-sectional area of an existing member will benefit that specific member by reducing the degree to which it is redundant to the system. However, this change will have a negative impact on the remaining members within the structure, as it will increase their level of redundancy within the system. It should also be emphasized that structural systems benefit from having redundant members. However, on one hand, a structural member can be completely redundant to the system, such as a column on top of the roof of a building carrying no loads and not supporting other members, and on the other hand, a member can be redundant but still contribute to the structural system, such as the double diagonal bar 6 in the truss shown in Fig. 3. Clearly, the distribution of material such that redundant members still add value to the system is more efficient. This does require achieving a balance between maximizing the redundancy of the system, while minimizing the redundancy of each member within the system.

5. Member redundancy index

One of the shortcomings of the previous analysis approach is that it takes no account of the range of DSI member j can gain between not having member i in the system and having it with $A_i = \infty$, namely $\delta_j^i(\infty)$. Such range of $\delta_j^i(\infty)$ can be larger for some members in some systems than others. One way to meaningfully account for such a range is to calculate a normalized measure of the amount gained in the DSI for a member due to the introduction of another member in the system. Accordingly, the MRI for member j w.r.t. introducing member i in the system, denoted as $\rho_j^i(A_i)$, is proposed as follows.

$$\rho_j^i(A_i) = \frac{\delta_j^i(A_i)}{\delta_j^i(\infty)} \times 100 \tag{17}$$

The MRI $\rho_j^i(A_i)$, as shown from Equation (17) is a relative measure of improvement in DSI for a member j caused by the presence, or introduction, of member i, that has an area A_i, to the system. By substituting Equations (12) and (13) in (17), the following can be obtained for calculating $\rho_j^i(A_i)$ as.

$$\rho_j^i(A_i) = \frac{\gamma_j^i(A_i) - \gamma_j^i(0)}{\gamma_j^i(\infty) - \gamma_j^i(0)} \times 100 \tag{18}$$

Similarly, the MRI for member i w.r.t. to itself being introduced in the system can be calculated as.

$$\rho_i^i(A_i) = \frac{\gamma_i^i(A_i) - \gamma_i^i(0)}{\gamma_i^i(\infty) - \gamma_i^i(0)} \times 100 \tag{19}$$

By using Equation (19), and recalling that $\gamma_i^i(0) = 1.0$ and $\gamma_i^i(\infty) = 0.0$, the following form for $\rho_i^i(A_i)$, can be obtained.

$$\rho_i^i(A_i) = \left[1 - \gamma_i^i(A_i)\right] \times 100 \tag{20}$$

Equation (20) shows that MRI for member i with A_i w.r.t. its own introduction in the system only depends on its DSI with A_i. To arrive at similar conclusions for other members in the system, one can substitute Equation (15) in Equation (17) and set $A_i = \infty$ in the denominator to obtain.

$$\rho_j^i(A_i) = \frac{\theta_j^i \delta_i^i(A_i)}{\theta_j^i \delta_i^i(\infty)} \times 100 \tag{21}$$

The constant θ_j^i can only be equal to 0 if member j has infinitely more stiffness than the remaining members in the system. By considering that such case is unlikely, θ_j^i can be cancelled out from Equation (21). By substituting Equations (12) and (13) in Equation (21), the following is obtained.

$$\rho_j^i(A_i) = \frac{\gamma_i^i(A_i) - \gamma_i^i(0)}{\gamma_i^i(\infty) - \gamma_i^i(0)} \times 100 \tag{22}$$

By using Equation (22), and recalling again that $\gamma_i^i(0) = 1.0$ and $\gamma_i^i(\infty) = 0.0$, the following form for $\rho_j^i(a)$, can be obtained.

$$\rho_j^i(A_i) = \left[1 - \gamma_i^i(A_i)\right] \times 100 \tag{23}$$

Comparing Equations (23) and (20) shows that.

$$\rho_j^i(A_i) = \rho_i^i(A_i) \tag{24}$$

Equations (20), (23), and (24) provide multiple important observations. First, the MRI for all members in the system will be the same w.r.t the presence, or introduction, of one of its members. At any value of A_i for member i, the relative improvement in DSI, i.e. $\rho_j^i(A_i)$, for all other members j is equal. Second, at any value of A_i for member i, the relative improvement in DSI for any member j, $\rho_j^i(A_i)$, is equal to the relative loss in DSI for member i, $\rho_i^i(A_i)$. Third, the relative measure of improvement, or loss, in DSI for any member in a system, due to the presence, or introduction of a member in the system, only depends on the DSI of member i. Fourth, since $\rho_j^i(A_i)$ and $\rho_i^i(A_i)$, only depend on the DSI of member i and are the same for all members in the system, the superscript is irrelevant and thus is dropped from the notation of the MRI from this point forward. These equations show that the MRI for each member in a system can be determined in a very simple manner. As explained in Equation (17), the MRI is a relative index, $\rho_i(A_i) = \rho_i^i(A_i) = \rho_j^i(A_i)$, expressed as a percentage, which varies between 0 % when $A_i = 0.0$ and 100 % when $A_i = \infty$ as shown in Fig. 2(c).

The MRI can shed some light on the relationship between the material distribution in the system and the distribution of redundancy and static indeterminacy. A repair regime for a system can benefit from such a concept to optimize the material usage in the system. It was explained that strengthening a member increases that member's DSI but decreases the DSI for the other members. Accordingly, when a member i is considered for repair or replacement, it may be of interest to provide a cross-sectional area to that member that provides a balanced relative improvement or deterioration in DSI of the members, i.e. provide A_i that causes $\rho_i(A_i)$ to be 50 %. Such target cross-sectional area can be denoted as τ_{50}^i, which satisfies the following equation.

$$\rho_i(\tau_{50}^i) = 50\% \tag{25}$$

By substituting Equation (25) in Equation (23), the following can be found.

$$\gamma_i^i(\tau_{50}^i) = 0.5 \tag{26}$$

Fig. 2(a) and (c) show τ_{50}^i, and the corresponding values in $\rho_i(a)$ and $\gamma_j^i(a)$, i.e., 50 % and 0.5, respectively. In a case in which certain reasons give rise to the importance of a member relative to the other members in the system, the target cross-sectional area of that member can be increased, say to τ_{90}^i, and the corresponding DSI and MRI can be obtained in a similar fashion.

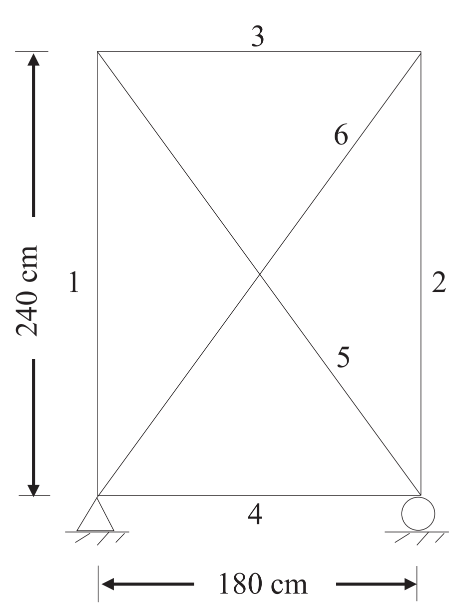

Fig. 3. An example of a statically indeterminate system to the 1st degree: A six-bar truss.

6. Application to statically determinate systems

Since the sum of the DSI values is the degree of static indeterminacy, such sum is 0 in statically determinate systems. In addition, DSI are strictly positive quantities. Accordingly, all values of $\gamma_i^i(A_i)$ and $\gamma_j^i(A_i)$ are zero in a statically determinate system. Therefore, the presented concepts of the MRI cannot be applied to statically determinate systems.

7. Application to a statically indeterminate system to the 1st degree

To analyze an example of a statically indeterminate structure to the 1st degree, the cross-sectional area for one of the members, A_i, in the six-bar truss shown in Fig. 3 is varied while maintaining the cross-sectional area of the remaining members $j \neq i$ at 1.0 cm^2. The modulus of elasticity for all members is 10,000 kN/cm^2.

Fig. 4(a) shows the reduction in DSI for member 1, $\gamma_1^1(A_1)$, as A_1 is increased. The vertical axis in the figure ends at 0.6 to provide visual clarity, even though $\gamma_1^1(0)$ is actually 1.0. The figure also shows how the DSI, $\gamma_j^1(A_1)$, for the remaining members increases, starting from 0.0, as $\gamma_1^1(A_1)$ decreases, starting from 1.0, when member 1 is introduced to the system. As a system that is indeterminate to the 1st degree in the presence of member 1, it is expected that $\gamma_j^1(0) = 0$, because the system without member 1 is determinate and $\sum_{j=2}^{6}\gamma_j^1(0) =$ the degree of static indeterminacy of the system without member 1, which is equal to 0 in this case, and $\gamma_j^1(0)$ cannot be negative. As A_i approaches infinity, each of the $\gamma_j^1(A_1)$ will reach a terminal value $\gamma_j^1(\infty)$, while $\gamma_1^1(A_1)$ arrives at $\gamma_1^1(\infty) = 0.0$. Interestingly, all the curves in the figure appear to flatten out after a certain value of A_i. In other words, the effect of increasing A_i tends to diminish as A_i approaches certain values. Therefore, the increase in A_i beyond some thresholds is clearly inefficient to the redundancy distribution in the system. Owing to the symmetry of members 5 and 6, their curves overlap. Similarly, the lowest curve in the figure presents the overlapping behavior of bars 3 and 4. Fig. 4(b) shows the reduction in DSI for member 2, $\gamma_2^2(A_2)$, starting from 1.0, as A_2 is increased, while the DSI for the remaining members, $\gamma_j^2(A_2)$, increases, starting from 0.0. It is interesting to observe from comparing Fig. 4(a)

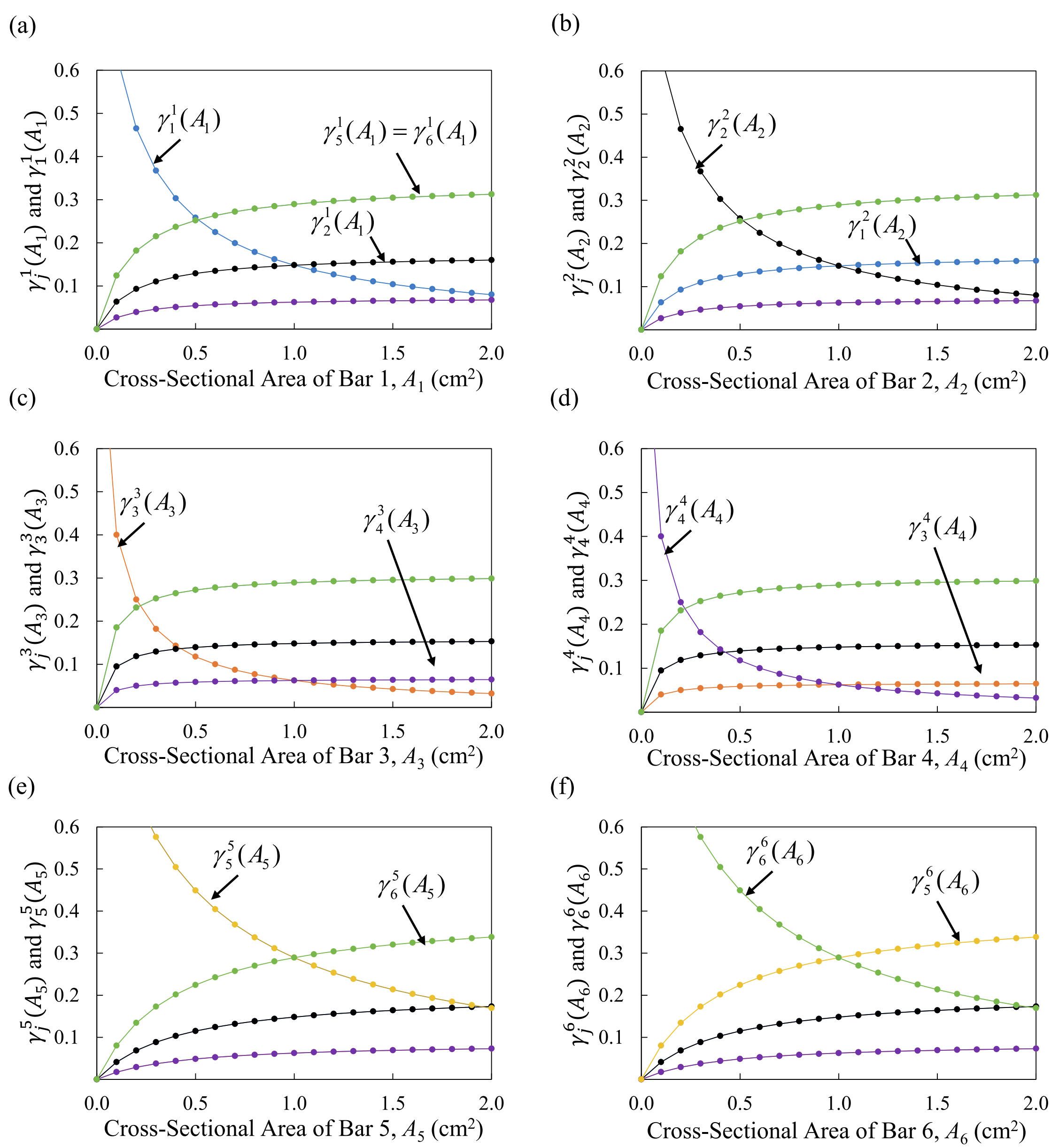

Fig. 4. The variation in DSI for all bars of the six-bar truss w.r.t the change in cross-section of members: (a) 1, (b) 2, (c) 3, (d) 4, (e) 5, and (f) 6.

and (b) how the curves for the two symmetrical members 1 and 2 switch in an identical manner, while the curves of the remaining members are the same in both figures. The same observations can be made for members 3 and 4 in Fig. 4(c) and (d), respectively, and members 5 and 6 in Fig. 4(e) and (f), respectively.

The values for $\rho_1^j(A_1)$ where also calculated for all members $j \neq 1$ using both Equations (18) and (23) and the results were found to be identical from both equations and for all bars. These results, represented as $\rho_1(A_1)$, are shown in Fig. 5(a). As expected, the MRI for all bars w.r.t. varying A_1 is the same as their curves overlap. As expected, the figure shows that $\rho_1(A_1)$ increases with A_1, starting from 0 % when $A_1 = 0.0$ and asymptotically approaches 100 % when A_1 approaches infinity. Moreover, the change in $\rho_1(A_1)$ tends to decrease as A_1 exceeds 1.6 cm^2, where $\rho_1(A_1) = 90$ %. However, $\rho_1(A_1) = 50$ % is reached at roughly $A_1 = 0.17$ cm^2. Therefore, $\tau_{90}^1 = 1.6$ cm^2 and $\tau_{50}^1 = 0.17$ cm^2. Depending on other conditions, such as the importance of member 1 to a certain loading case, a target cross-sectional area of τ_T^1 can be adopted in order to determine the cross-sectional area of a member that is required to be repaired or replaced whenever necessary. Fig. 5(b) shows the variation in the MRI of the members as the cross-sectional area of that member is varied from 0.0 to 2.0. For instance, the curve for $\rho_2(A_2)$ shows the variation in the MRI of Member 2 as its cross-sectional area is varied from 0.0 to 2.0. As expected, due to symmetry, $\rho_1(A_1)$ and $\rho_2(A_2)$ are identical. The same observation can be made in Fig. 5(b) for $\rho_3(A_3)$ and $\rho_4(A_4)$ that are identical and $\rho_5(A_5)$ and $\rho_6(A_6)$ that are also identical. The choice to end the curves at 2.0 is purely based on the visual clarity of the figures that this provides. As explained in Fig. 2(c), all MRIs approach 100 % when the cross-sectional area of the member is $A_i = \infty$.

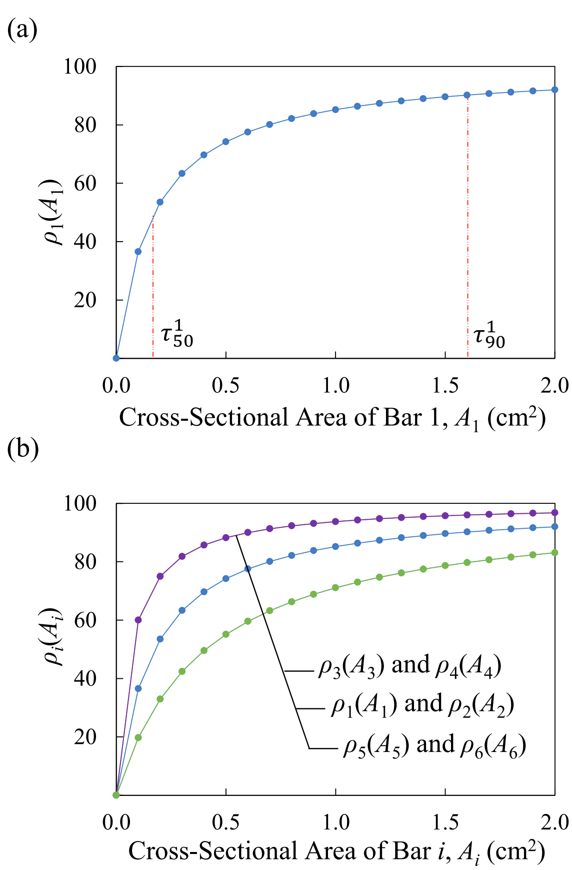

Fig. 5. The variation in MRI in the six-bar truss w.r.t the change in cross-section of members: (a) 1, and (b) all bars.

8. Application to statically indeterminate system to the 2nd degree

As an example of a statically indeterminate system to the second degree, the 4-cable-1-strut 3D system adopted from Maurin *et al.* [32] and shown in Fig. 6 is considered. Member 5 is a compression strut, while the remaining members are cables. The cross-sectional area for one of the members, A_i, is varied while maintaining the cross-sectional area of the remaining members at 1.0 cm^2. The modulus of elasticity for all members is 10,000 kN/cm^2.

Fig. 7(a) through (e) show the variation in DSI for members 1 through 5, as the cross-sectional areas A_1 through A_5, are increased, respectively. In each of these curves, it is clear that when the cross-sectional area of a member is increased from 0 onward, its DSI decreases from 1.0 downward. It should be noted that the analysis, although not shown in the figures, did affirm that when the cross-sectional area of a member approaches infinity, the DSI for that member approaches zero. On the other hand, while the DSI decreases for a member whose cross-sectional area increases, the DSI for the remaining members increases. However, unlike in the previous example, the figure shows that when the cross-sectional area of a member is zero, the DSI for the remaining members is not necessarily zero. As an indeterminate system to the second degree, when the cross-sectional area of a member, i, is 0, the sum of the DSI's for the remaining members must be 1.0 in order to satisfy $\sum_{j\neq i}^{5}\gamma_j^i(0)$ = the degree of static indeterminacy of the system without member i, which is 1.0. Interestingly, the DSI of member 4 starts at 0.0 when $A_3 = 0$ in Fig. 7(c), and the DSI of member 3 starts at 0.0 when $A_4 = 0$ in Fig. 7(d). This can be attributed to the fact that the absence of member 4 provides freedom of elongation to member 3, and vice versa. Due to the symmetry between members 1 and 2, the behavior of the DSI curves for each of members 3, 4, and 5 is identical in Fig. 7(a) to their counterparts in Fig. 7(b). In other words, the effect of increasing the cross-sectional area of member 1 on the restraint of members 3, 4 and 5 is the same as the effect of increasing the cross-sectional area of member 2. Furthermore, in Fig. 7(c), (d), and (e), the curves of members 1 and 2 overlap. Fig. 7(c) and (d) show that varying the cross-sectional area of neither member 3 nor 4 has any effect on the DSI of members 1 and 2 as it is constant throughout both figures. Moreover, Fig. 7(e) clearly shows that the variation of the cross-sectional area of member 5 has no bearing on the DSI's of members 3 and 4, because the elongation

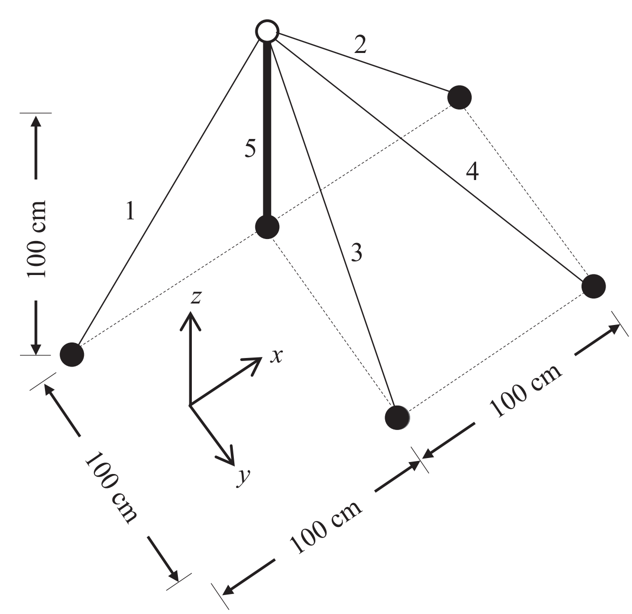

Fig. 6. An example of a statically indeterminate system to the 2nd degree: 4-cable-1-strut 3D system.

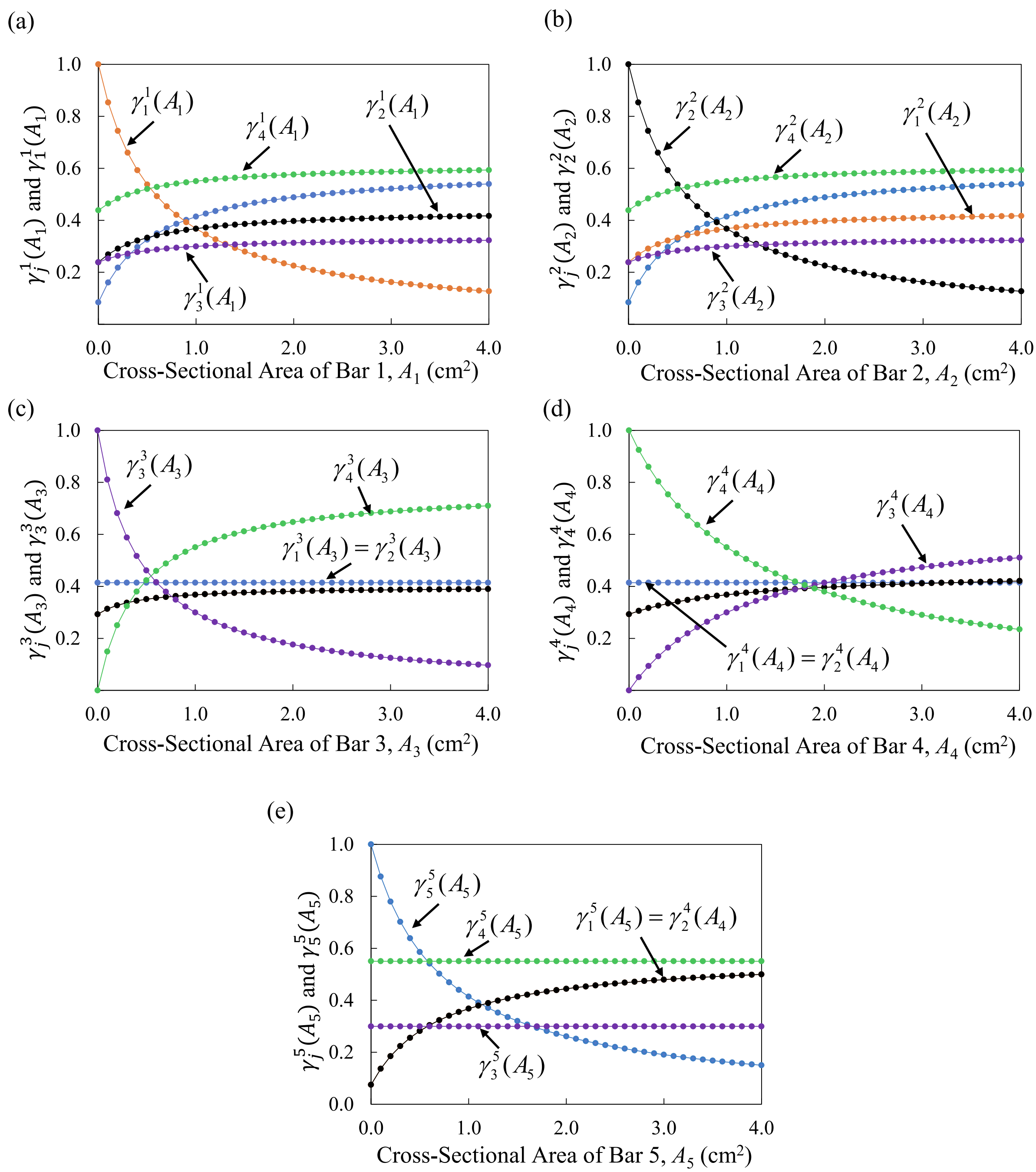

Fig. 7. The variation in DSI for all bars of the 4-cable-1-strut 3D system w.r.t the change in cross-section of members: (a) 1, (b) 2, (c) 3, (d) 4, and (e) 5.

of either members 3 or 4 will only cause a free body rotation of member 5. If members 1 or 2 were not present in the system, then elongation of either member 3 or member 4 will cause free body rotation of member 5 without any resistance. In the presence of members 1 and 2, the elongation of either members 3 or 4 will cause member 5 to rotate freely around the *x*-axis. The only resistance to the elongation of members 3 and 4 will come from either each other or from members 1 and 2, which is confirmed by Fig. 7. This can also be confirmed by noticing that the off-diagonal elements of the redundancy matrix that relate the constraint of member 5 to members 3 and 4 are $R_{5,3} = R_{5,4} = R_{3,5} = R_{4,5} = 0.0$. An off-diagonal element $R_{i,j}$ in the redundancy matrix is an indicator of the effect of an initial elongation in element j on element i [10].

Fig. 8 shows the variation in each of the MRI's, $\rho_i(A_i)$, in the system as A_i varies. As expected, each $\rho_i(A_i)$ increases from 0 % to 100 % as A_i increases from zero to infinity. However, the increase in $\rho_i(A_i)$ begins to slow down rapidly as A_i increases.

9. Application to statically indeterminate system to the 24th degree

The 72-bar 3D truss shown in Fig. 9 is analyzed as an example of an indeterminate structure with a high degree of indeterminacy, namely 24. Due to the large number of members in the structure, the MRI w.r.t only two members, namely 1 and 35 will be considered as an example. The cross-sectional area for each of members 1 and 35, A_1 and A_{35}, are varied, respectively, while maintaining the cross-sectional area of the remaining members at 1.0 cm^2. The modulus of elasticity for all members is 200,000 MPa.

Fig. 10(a) and (b) show the variation in DSI for all the members in the

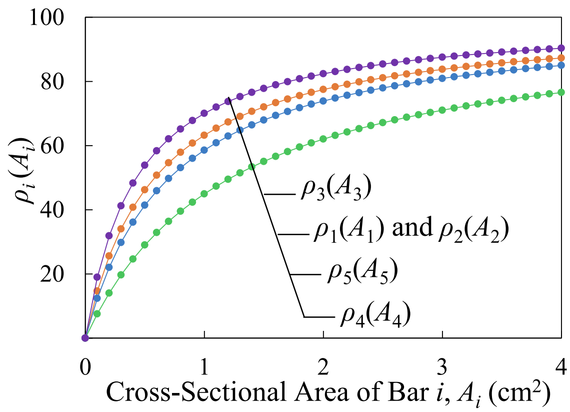

Fig. 8. The variation in MRI in the 4-cable-1-strut 3D system w.r.t the change in cross-section of member i, A_i.

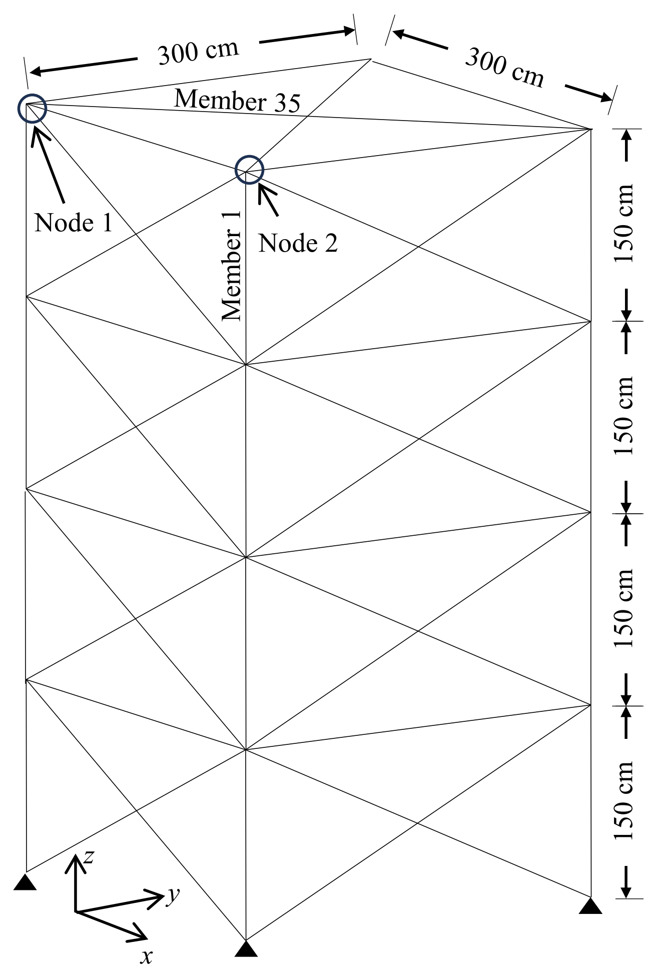

Fig. 9. An example of a statically indeterminate system to the 24th degree: A 72-bar 3D truss.

truss, as A_1 and A_{35}, are increased, respectively. The vertical axis in the figure is terminated at 0.6 to provide visual clarity, even though $\gamma_1^1(0)$, $\gamma_{35}^{35}(0)$ are actually 1.0. Once again, the figures clearly show the inverse relationship between the DSI of the member with an increasing cross-sectional area and the DSI of the remaining members in the system. However, it is clear from both figures that the variation in the DSI of the remaining members in such a system with large numbers of members is very small compared to the variation noticed in the systems with fewer

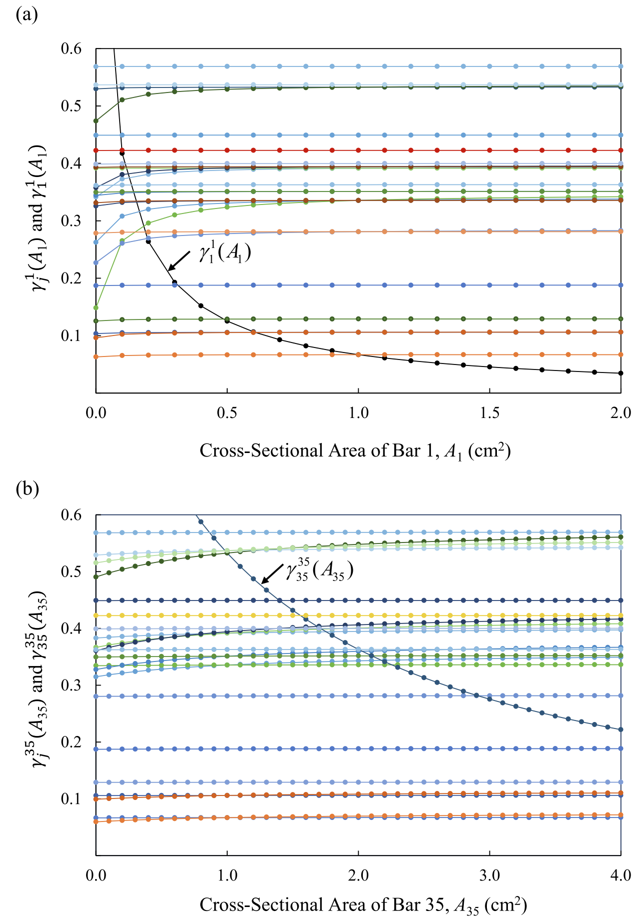

Fig. 10. The variation in DSI for all bars of the 72-bar 3D truss w.r.t the change in cross-section of members: (a) 1, and (b) 35.

members. This is because the loss in DSI in the member with the increasing cross-sectional area is distributed in this system to a large number of members, and therefore the share for each of these members is small compared to systems with fewer members. At the start of the curves, where the decline in DSI is most pronounced, there appears to be some improvement in a small number of adjacent members. These members are located near the member where the cross-sectional area has been increased, and whose restraint is affected the most by such cross-sectional area increase.

Fig. 11 shows the variation in each of the MRI's w.r.t members 1 and 35, $\rho_1(A_1)$ and $\rho_{35}(A_{35})$, as A_1 and A_{35} vary, respectively. As usual, each MRI increases from 0 % to 100 % as A_i increases from zero to infinity. However, the increase in $\rho_i(A_i)$ begins to slow down rapidly as either A_1 or A_{35} increases. The figure shows that the 50 % target area for member 35, $\tau_{50}^{35} = 1.05$ cm^2 and the 90 % target area for member 1 is only$\tau_{90}^{1} = 0.65$ cm^2.

The MRI can be incorporated into an automated design optimization process in order to achieve an efficient material allocation that provides an optimum spatial redundancy distribution. Moreover, the MRI can be incorporated into reliability-based design optimization problems. One way to achieve this goal is to impose constraints in the optimization problem formulation with minimum MRI values allowed for the members in the system. In this 72-bar truss example, this can be accomplished with the following simple design optimization problem formulation.

minimize:

$$V = \sum_{1}^{72} A_i L_i$$

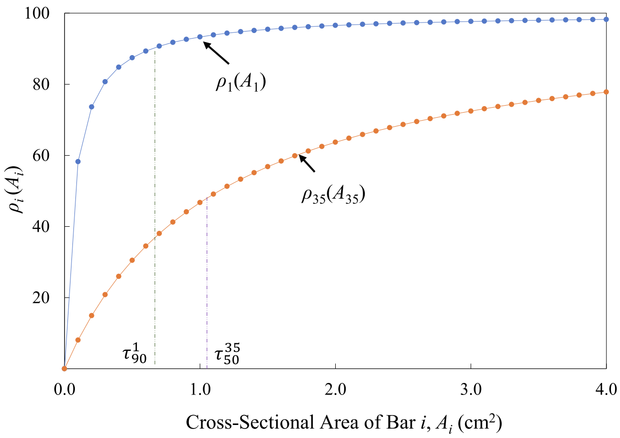

Fig. 11. The variation in MRI in the 72-bar 3D truss w.r.t the change in cross-section of members 1 and 35.

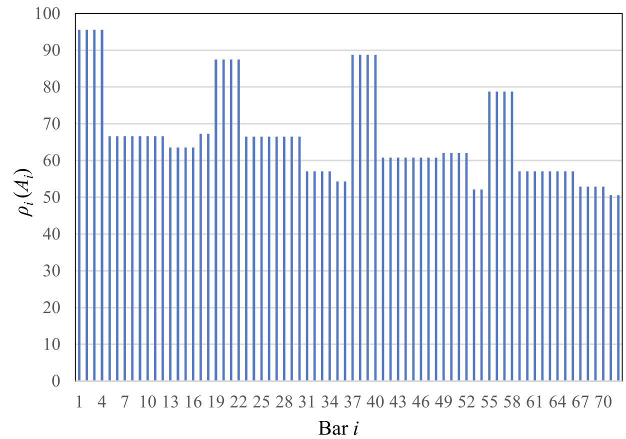

Fig. 12. Values of the MRI for the optimally designed members of the 72-bars truss.

subject to:

$\rho_i(A_i) > 50.0$ for all $i \in \{1, 2,.., 72\}$.

$\beta_{sys} > 3.0$

where V is the total volume of the truss, L_i is the length of member i, where the minimum allowed value of the MRI is 50 for all members, and β_{sys} is the system reliability index for the truss with a set minimum value of 3.0. In this problem, the 72 bars are assigned into 16 groups. Accordingly, there are 16 design variables such that each design variable represents the cross-sectional area of the members in one of the groups. These design variables are discrete and can only take one of the following values {0.1; 0.3; 0.5; 0.7; 0.9; 1.1; 1.3; 1.5; 1.7; 1.9; 2.1; 2.3; 2.5; 2.7; 2.9; 3.1; 3.3; 3.5; 3.7; 3.9; 4.1; 4.3; 4.5} cm^2. The nodal coordinates, member connectivity, and group assignment for this problem can be found in Okasha [33]. The truss is subjected to two load effects acting on nodes 1 and 2 in the y direction. Nodes 1 and 2 are located at the top of the truss as shown in Fig. 9. The applied forces are treated as statistically independent normally distributed random variables with mean and coefficient of variation of 5 kN and 15 %, respectively. The moduli of elasticity of the bars are also treated as normally distributed random variables with mean and coefficient of variation of 200,000 MPa and 15 %, respectively. Table 1 shows the solution obtained for the areas of each group. The total volume of the optimum truss is 5841.5 cm^3 and its system reliability index is 3.46. Fig. 12 shows the MRI for each member in the truss. Within each group, the MRI is the same for the members of that group. It is clear from the figure that incorporating the MRI into the optimization problem formulation has guided the solution into delivering an efficient allocation of material with a good special redundancy distribution.

Table 1
Solution of the design optimization problem for the 72-bar truss.

Group *id*	Cross Sectional Area (cm^2)
1	1.1
2	0.7
3	0.5
4	0.9
5	0.7
6	0.9
7	0.7
8	1.1
9	0.9
10	0.7
11	0.9
12	1.1
13	0.7
14	0.9
15	0.7
16	1.1

10. Conclusions

To ensure an efficient distribution of material in a system, proper quantification of its effect on structural redundancy is essential. The common measures of redundancy, powerful as they are, do not provide insight into the spatial distribution of redundancy in the system. In this paper, the member redundancy index was derived as a means to achieve this goal. The logic for deriving this indicator is built upon concepts of the redundancy matrix, and its byproduct of distributed static indeterminacy.

It was found that the MRI is capable of providing a logical means for measuring the level of redundancy built into structural members, due to the presence of one of these members, relative to the loss of that member. The MRI is a function of the cross-sectional area of the structural member in question. Therefore, it offers a convenient instrument for the optimization of material distribution in a system.

Several examples were analyzed using the MRI, and the results indicated that the MRI values for a given member are identical across all members within the system. These results, also show that the MRI increases with the increase in the cross-sectional area of the member in question, starting from 0 % when the cross-sectional area of that member is 0.0 and asymptotically approaches 100 % when the cross-sectional area approaches infinity. Moreover, the change in MRI tends to diminish as the cross-sectional area of the member in question exceeds a certain value. Depending on other factors, such as the member's significance in a particular loading scenario, a specific target area may be selected to determine the required cross-sectional area of a member that should be repaired or replaced.

This study shows the results based on the cross-sectional area between 0 and infinity for illustrative purposes. For practical applications, the minimum and maximum cross-sectional areas of members should be determined based on the design requirements and loading conditions. The approach presented here is specifically aimed at analyzing structural systems consisting of axial members. Further investigations are still needed to apply the proposed approach to other types of structures.

CRediT authorship contribution statement

Nader M. Okasha: Conceptualization, Methodology, Software, Writing – original draft, Funding acquisition. **Mohamed Soliman:** Validation, Investigation. **Sunyong Kim:** Validation, Visualization. **Dan M. Frangopol:** Supervision, Validation, Writing – review & editing. **Abdel Kareem Alzo'ubi:** Writing – review & editing.

Declaration of Competing Interest

The authors declare that they have no known competing financial interests or personal relationships that could have appeared to influence the work reported in this paper.

Data availability

No data was used for the research described in the article.

Acknowledgement

The authors acknowledge financial support from Abu Dhabi University's Office of Research and Sponsored Programs. Grant number: 19300798.

References

[1] Okasha NM, Frangopol DM. Novel approach for multi-criteria optimization of life-cycle preventive and essential maintenance of deteriorating structures. *J Struct Eng*, ASCE 2010;136(8):1009–22. https://doi.org/10.1061/(ASCE)ST.1943-541X.0000198.
[2] Okasha NM, Frangopol DM. Redundancy of structural systems with and without maintenance: An approach based on lifetime functions. *Reliab Eng Syst Saf*, Elsevier 2010;95(5):520–33. https://doi.org/10.1016/j.ress.2010.01.003.
[3] Okasha NM, Frangopol DM. Time-variant redundancy of structural systems. *Struct Infrastruct Eng*, Taylor & Francis 2010;6(1–2):279–301. https://doi.org/10.1080/15732470802664514.
[4] Okasha NM, Frangopol DM. Lifetime-oriented multi-objective optimization of structural maintenance considering system reliability, redundancy and life-cycle cost using GA. *Struct Saf*, Elsevier 2009;31(6):460–74. https://doi.org/10.1016/j.strusafe.2009.06.005.
[5] Okasha NM. System Reliability Based Multiobjective Design Optimization of Bridges. *Struct Eng Int*, Taylor & Francis 2016;26(4):324–32. https://doi.org/10.2749/101686616X14555429843726.
[6] Pandey PC, Barai SV. Structural sensitivity as a measure of redundancy. *J Struct Eng*, ASCE 1997;123(3):360–4. https://doi.org/10.1061/(ASCE)0733-9445(1997)123:3(360).
[7] Frangopol DM, Curley JP. Effects of damage and redundancy on structural reliability. *J Struct Eng*, ASCE 1987;113(7):1533–49. https://doi.org/10.1061/(ASCE)0733-9445(1987)113:7(1533).
[8] Maxwell JC. On the calculation of the equilibrium and stiffness of frames. *London, Edinburgh, and Dublin Philos Mag J Sci*, Taylor & Francis 1864;27:294–9. https://doi.org/10.1080/14786446408643668.
[9] Pellegrino S, Calladine CR. Matrix analysis of statically and kinematically indeterminate frameworks. *Int J Solids Struct*, Elsevier 1986;22:409–28. https://doi.org/10.1016/0020-7683(86)90014-4.
[10] Scheven MV, Ramm E, Bischoff M. Quantification of the redundancy distribution in truss and beam structures. *Int J Solids Struct*, Elsevier 2021;213:41–9. https://doi.org/10.1016/j.ijsolstr.2020.11.002.
[11] Zhou Jy, Chen Wj, Zhao B, Qiu Zy, Dong Sl. Distributed indeterminacy evaluation of cable-strut structures: formulations and applications. *J Zhejiang Univ-Sci A*, Springer, 2015 ;(16)9, 737–748. https://doi.org/10.1631/jzus.A1500081. URL: https://link.springer.com/article/10.1631/jzus.A1500081.
[12] Guest SD. The stiffness of tensegrity structures. *IMA J Appl Math*, Oxford Academic 2011;76(1):57–66. https://doi.org/10.1093/imamat/hxq065.
[13] Chen Y, Sareh P, Feng J. Effective insights into the geometric stability of symmetric skeletal structures under symmetric variations. *Int J Solids Struct*, Elsevier 2015; 69–70:277–90. https://doi.org/10.1016/j.ijsolstr.2015.05.023.
[14] Chen Y, Feng J, Lv H, Sun Q. Symmetry representations and elastic redundancy for members of tensegrity structures. *Compos Struct*, Elsevier 2018;203:672–80. https://doi.org/10.1016/j.compstruct.2018.07.044.
[15] Linkwitz K. *Error theory and adjustment of networks according to the theory of elastic systems.* Ph.D. Thesis. Bavarian Academy of Sciences and Humanities, Munich; 1961.
[16] Ströbel D, Singer P. *Recent developments in the computational modelling of textile membranes and inflatable structures*. In: Oñate, E., Kröplin, B. (Eds) Textile Composites and Inflatable Structures II. Computational Methods in Applied Sciences, vol 8. Springer, Dordrecht; 2008.
[17] Wagner R. On the design process of tensile structures. Netherlands: Springer; 2005.
[18] Tibert AG. Distributed indeterminacy in frameworks. *Proceedings of the 5th International Conference on Computation of Shell and Spatial Structures*, Salzburg, Austria; 2005.
[19] Tibert, A.G. (2005). Flexibility evaluation of prestressed kinematically indeterminate frameworks. The 18th Nordic Seminar on Computational Mechanics, Helsinki, Finland.
[20] Eriksson A, Tibert AG. Redundant and force differentiated systems in engineering and nature. *Comput Methods Appl Mech Eng*, Elsevier 2006;195(41–43):5437–53. https://doi.org/10.1016/j.cma.2005.11.007.
[21] Chen Q, Kou XJ, Zhang Y. Internal force and deformation matrixes and their applications in load path. *J Zhejiang Univ-SCIENCE A*, Springer 2010;11(8):563–70. https://doi.org/10.1631/jzus.A0900630.
[22] Gao Y, Liu XL. Weighted graph form of structures and its application in robustness analysis. *J Shanghai Jiaotong Univ (Science)*, Springer 2013;18)2:216–23. https://doi.org/10.1007/s12204-013-1385-2.
[23] Jiang M, Kou XJ, Li ZM. The redundancy matrix of rigid-frame structure and its application. URL J Donghua Univ 2012;29:107–10. http://www.cqvip.com/qk/86692x/20122/42710319.html.
[24] Kolakowski P, Wiklo M, Holnicki-Szulc J. The virtual distortion method – a versatile reanalysis tool for structures and systems. *Struct Multidiscip Optim*, Springer 2008;36:217–34. https://doi.org/10.1007/s00158-007-0158-7.
[25] Kou X, Chen Q, Song J. Reliability estimation involving indirect load effects. In: Kong H, editor. Proceeding of the 4th Asian-Pacific Symposium; 2008. p. 137–40.
[26] Chen Q, Kou XJ. A constraint matrix approach for structural ultimate resistance to access the importance coefficient values of rigid joints. *Adv Struct Eng*, Sage 2013; 16(11):1863–70. https://doi.org/10.1260/1369-4332.16.11.1863.
[27] Krake T, von Scheven M, Gade J, Abdelaal M, Weiskopf D, Bischoff M. Efficient update of redundancy matrices for truss and frame structures. *Journal of Theoretical, Computational and Applied Mechanics*, JTCAM, November 2022, 1-19 https://doi.org/10.46298/jtcam.9615. URL: https://jtcam.episciences.org/10398.
[28] Gade J, Tkachuk A, von Scheven M, Bischoff M. A continuum-mechanical theory of redundancy in elastostatic structures. *Int J Solids Struct*, Elsevier 2021;110977: 226–7. https://doi.org/10.1016/j.ijsolstr.2021.01.022.
[29] Zhao B, Hu J, Chen W, Chen J, Qiu Z, Jing Z. Computational method for in-situ finite element modeling of inflatable membrane structures based on geometrical shape measurement using photogrammetry. *Comput Struct*, Elsevier 2019;224: 106105. https://doi.org/10.1016/j.compstruc.2019.106105.
[30] Gan BS. Computational modeling of tensegrity structures. Springer International Publishing; 2020.
[31] Wang Y, Senatore G. Extended integrated force method for the analysis of prestress-stable statically and kinematically indeterminate structures. *Int J Solids Struct*, Elsevier 2020;202:798–815. https://doi.org/10.1016/j.ijsolstr.2020.05.029.
[32] Maurin B, Bagneris M, Motro R. Mechanisms of prestressed reticulate systems with unilateral stiffened components. *Eur J Mech A Solids*, Elsevier 2008;27(1):61–8. https://doi.org/10.1016/j.euromechsol.2007.05.009.
[33] Okasha NM. Proposed Algorithms for an Efficient System-Reliability Based Design Optimization of Truss Structures. *J Comput Civ Eng*, ASCE 2016;30(5), CID: 04016008. https://doi.org/10.1061/(ASCE)CP.1943-5487.0000569.